World Academy of Science, Engineering and Technology
International Journal of Mechanical and Mechatronics Engineering
Vol:6, No:8, 2012

Analysis of Short Bearing in Turbulent Regime Considering Micropolar Lubrication

S. S. Gautam*, S. Samanta

***Abstract*—**The aim of the paper work is to investigate and predict the static performance of journal bearing in turbulent flow condition considering micropolar lubrication. The Reynolds equation has been modified considering turbulent micropolar lubrication and is solved for steady state operations. The Constantinescu's turbulence model is adopted using the coefficients. The analysis has been done for a parallel and inertia less flow. Load capacity and friction factor have been evaluated for various operating parameters.

***Keywords*—**hydrodynamic bearing, micropolar lubrication, coupling number, characteristic length, perturbation analysis

I. Introduction

TURBULENT flow conditions often prevail in high-speed bearings. Therefore, evaluation of performances of bearings operating in turbulent flow regime has always been concern of engineers and researchers [1-5]. Turbulent flow is characterized by increased viscosity and shear stress. To calculate bearing performance several researchers viz. Constantinescu [1], Ng and Pan [2], Elrod and Ng [3] presented various models and developed Reynolds equation for turbulent lubrication of bearings. Constantinescu [1] employed Prandtl mixing length hypothesis, Ng and Pan [2] and Elrod and Ng [3] used the concept of Reichardt's eddy diffusivity. Taylor and Dowson [4] suggested the application of the then existing lubrication theories given by Ng, Pan and Elrod. Ghosh and Nagraj [5] have studied the rotordynamic characteristics for hybrid bearing. The references are restricted in numbers for turbulent analysis due to space limitation.

The adoption of non Newtonian fluids has been increased in lubrication during the last two decades. The microfluid was considered to contain microstructures which can translate, rotate and deform independently. The micropolar fluid considers the microrotational effects ignoring the microdeformation effects. The theory included the translation velocities and angular or spin velocities of the microstructures. Many researchers [6 - 10] have studied the problem of laminar lubrication condition using micropolar fluid. The aspect of turbulent lubrication considering micropolar fluid is still having a great scope to work about. The authors focus this aspect and try to analyze the performances.

II. Derivation of Governing Equations

The circular bearing geometry is shown in Fig.1. The variation of the film thickness along the circumference of a journal bearing is

$$\bar{h} = \frac{h}{C} = 1.0 + \varepsilon \cos\theta \tag{1}$$

where, θ is the angular coordinate starting from the line of centers .

When the film oil is a non Newtonian fluid, the Reynolds equation can still be successfully used by means of some modifications for turbulent micropolar lubrication. One possible way of taking into account the influence of the non Newtonian behavior is the introduction of the micropolar function in the Reynolds equation by Faralli and Belfiore [11].

The dimensional Reynolds equation is as follows:

$$\frac{\partial}{\partial x}\left(\frac{h^3\phi(\Lambda,N,h)}{\mu}\frac{\partial p}{\partial x}\right)+\frac{\partial}{\partial z}\left(\frac{h^3\phi(\Lambda,N,h)}{\mu}\frac{\partial p}{\partial z}\right) = \frac{U}{2}\frac{\partial h}{\partial x}+\frac{\partial h}{\partial t} \tag{2}$$

where,

$$\phi(\Lambda,N,h) = \frac{1}{K_{x,z}}+\frac{\Lambda^2}{h^2}-\frac{N\Lambda}{2h}\coth\left(\frac{Nh}{2\Lambda}\right) \tag{3}$$

The Reynolds equation has been non dimensionalised as

$$\frac{\partial}{\partial\theta}\left(\phi\left(N,l_m,\bar{h}\right)\frac{\partial\bar{p}}{\partial\theta}\right)+\left(\frac{D}{L}\right)^2\frac{\partial}{\partial\zeta}\left(\phi\left(N,l_m,\bar{h}\right)\frac{\partial\bar{p}}{\partial\zeta}\right) = \frac{1}{2}\frac{\partial\bar{h}}{\partial\theta}+\gamma\frac{\partial\bar{h}}{\partial\tau} \tag{4}$$

where,

$$\bar{\phi}\left(N,l_m,\bar{h}\right) = \frac{\bar{h}^3}{K_{\theta,\zeta}}+\frac{\bar{h}}{l_m^2}-\frac{N\bar{h}^2}{2l_m}\coth\left(\frac{Nl_m\bar{h}}{2}\right) \tag{5}$$

$$\theta=\frac{x}{R},\zeta=\frac{2z}{L},\quad \bar{p}=\frac{pC^2}{\mu\omega R^2},\ \bar{h}=\frac{h}{C},\ \tau=\omega t$$

For short bearing assumption the above equation modifies to

$$\left(\frac{D}{L}\right)^2\frac{\partial}{\partial\zeta}\left(\phi\left(N,l_m,\bar{h}\right)\frac{\partial\bar{p}}{\partial\zeta}\right)=\frac{1}{2}\frac{\partial\bar{h}}{\partial\theta}+\gamma\frac{\partial\bar{h}}{\partial\tau} \tag{6}$$

γ is whirl ratio. The turbulent shear coefficient determined following Taylor and Dowson [4] as given below:

S. S. Gautam and S. Samanta are with Mechanical Engineering Department, North Eastern Regional Institute of Science and Technology, Itanagar, India, [*satyam.gautam@gmail.com].

$$K_\zeta = 12 + 0.0088\,\mathrm{Re}_h^{\,0.88} \tag{7}$$

Where, $\mathrm{Re}_h = \bar{h}\,\mathrm{Re}$, $\mathrm{Re} = \rho C R\omega/\mu$ is Reynolds number and $10000 \geq \mathrm{Re} \geq 5000$ for turbulent flows.

The steady-state and dynamic performance can be evaluated by using a small amplitude perturbation technique. Under dynamic conditions the equilibrium position of the journal centre defined by parameters ε_0 and ϕ_0 is perturbed by a small motion.

Relatively, the instantaneous position of the bearing center is defined by

$$\begin{cases} \varepsilon = \varepsilon_0 + \varepsilon_1, & \varepsilon_1 << \varepsilon_0 \\ \phi = \phi_0 + \phi_1, & \phi_1 << \phi_0 \end{cases} \tag{8}$$

where the variables ε_1 and ϕ_1 are assumed to be small compared to ε_0 and ϕ_0 .Using above equations, the perturbed dimensionless film thickness, turbulent coefficient and pressure are as given below following Ghosh & Nagraj [5] and Meena et. al. [12].

$$\begin{cases} \bar{h} = \bar{h}_0 + \varepsilon_1 \cos\theta + \varepsilon_0\phi_1 \sin\theta \\ K_\zeta = K_{\zeta 0} + \varepsilon_1 K_{\zeta 1} + \varepsilon_0\phi_1 K_{\zeta 2} \\ \bar{p} = \bar{p}_0 + \bar{p}_1\varepsilon_1 + \bar{p}_2\varepsilon_0\phi_1 + \bar{p}_3\dot{\varepsilon}_1 + \bar{p}_4\varepsilon_0\dot{\phi}_1 \end{cases} \tag{9}$$

Introducing equations (9) into the Reynolds equation (6) and retaining terms of zero and first order only a system of five differential equations are obtained using short bearing approximation as given below.

$$C_1 \frac{\partial^2 \bar{p}_0}{\partial\zeta^2} = \left(\frac{L}{D}\right)^2 \frac{1}{2}\frac{\partial \bar{h}_0}{\partial\theta} \tag{10}$$

$$C_1 \frac{\partial^2 \bar{p}_1}{\partial\zeta^2} + C_2 \frac{\partial^2 \bar{p}_0}{\partial\zeta^2} = -\left(\frac{L}{D}\right)^2 \frac{1}{2}\sin\theta \tag{11}$$

$$C_1 \frac{\partial^2 \bar{p}_2}{\partial\zeta^2} + C_3 \frac{\partial^2 \bar{p}_0}{\partial\zeta^2} = \left(\frac{L}{D}\right)^2 \frac{1}{2}\cos\theta \tag{12}$$

$$C_1 \frac{\partial^2 \bar{p}_3}{\partial\zeta^2} = \left(\frac{L}{D}\right)^2 \gamma\cos\theta \tag{13}$$

$$C_1 \frac{\partial^2 \bar{p}_4}{\partial\zeta^2} = \left(\frac{L}{D}\right)^2 \gamma\sin\theta \tag{14}$$

where, $C_1 = \left[\frac{\bar{h}^3}{K_\zeta} + \frac{\bar{h}}{l_m^2} - \frac{N\bar{h}^2}{2l_m}\coth\left(\frac{Nl_m\bar{h}}{2}\right)\right]$,

$$C_2 = \left[\frac{3\bar{h}_0^2\cos\theta}{K_{\zeta_0}} - \frac{\bar{h}_0^3 K_{\zeta_1}}{K_{\zeta_0}^2} + \frac{\cos\theta}{l_m^2}\right.$$

$$\left. - \frac{N\bar{h}_0\cos\theta}{l_m}\coth\left(\frac{Nl_m\bar{h}_0}{2}\right) + \frac{N^2\bar{h}_0^2\cos\theta}{4}\cos ec^2 h\left(\frac{Nl_m\bar{h}_0}{2}\right)\right]$$

$$\&\quad C_3 = \left[\frac{3\bar{h}_0^2\sin\theta}{K_{\zeta_0}} - \frac{\bar{h}_0^3 K_{\zeta_2}}{K_{\zeta_0}^2} + \frac{\sin\theta}{l_m^2}\right.$$

$$\left. - \frac{N\bar{h}_0\sin\theta}{l_m}\coth\left(\frac{Nl_m\bar{h}_0}{2}\right) + \frac{N^2\bar{h}_0^2\sin\theta}{4}\cos ec^2 h\left(\frac{Nl_m\bar{h}_0}{2}\right)\right]$$

Atmospheric pressure is assumed at the two bearing ends. For circular journal bearings, equations (10) to (14) must satisfy the boundary conditions at two bearing ends, a periodic condition and cavitation must be used.

$$\begin{cases} p_{\theta=0} = p_{\theta=2\pi} \quad ; & \text{For periodicity} \\ \bar{p}(\theta, \pm 1) = 0 \quad ; & \text{Pressures at ends} \\ \dfrac{\partial \bar{p}}{\partial\theta}(\theta_{cav}, \zeta) = 0, \quad \bar{p}(\theta, \zeta) = 0, & for\ \theta \geq \theta_{cav} \end{cases} \tag{15}$$

The static and dynamic pressures are calculated by integrating equations (10) to (14) satisfying above boundary conditions at the bearing ends and for γ=1.

$$\bar{p}_0 = \frac{\varepsilon_0 \sin\theta}{4C_1}\left(\frac{L}{D}\right)^2\left[1-\zeta^2\right] \tag{16}$$

$$\bar{p}_1 = \frac{\sin\theta}{4C_1}\left(\frac{L}{D}\right)^2\left(1 - \varepsilon_0\frac{C_2}{C_1}\right)\left[1-\zeta^2\right] \tag{17}$$

$$\bar{p}_2 = -\frac{1}{4C_1}\left(\frac{L}{D}\right)^2\left(\varepsilon_0\sin\theta\frac{C_3}{C_1} + \cos\theta\right)\left[1-\zeta^2\right] \tag{18}$$

$$\bar{p}_3 = -\frac{\gamma\cos\theta}{2C_1}\left(\frac{L}{D}\right)^2\left[1-\zeta^2\right] \tag{19}$$

$$\bar{p}_4 = -\frac{\gamma\sin\theta}{2C_1}\left(\frac{L}{D}\right)^2\left[1-\zeta^2\right] \tag{20}$$

III. Static Characteristics

The radial and tangential components of the resulting load are computed as:

Dimensionless radial component of load is:

$$\overline{W}_r = -2\int_0^{L/2}\int_0^{2\pi} \bar{p}_0\cos\theta\, d\theta\, d\zeta \tag{21}$$

Dimensionless tangential component of load is:

$$\overline{W_t} = 2\int_0^{L/2}\int_0^{2\pi} \overline{p}_0 \sin\theta d\theta d\zeta \tag{22}$$

The resultant radial load on the bearing is (dimensionless) written as:

$$\overline{W} = \sqrt{\overline{W}_r{}^2 + \overline{W}_t{}^2} \tag{23}$$

The dimensionless friction force is given as follows for short bearing Das et. al. [7]:

$$\overline{F} = 2\int_0^{L/2}\int_0^{\theta_{cav}} A d\theta\, d\zeta + 2\int_0^{L/2}\int_{\theta_{cav}}^{2\pi} A\frac{\overline{h}_{cav}}{\overline{h}} d\theta\, d\zeta \tag{24}$$

where,
$$A = \frac{\overline{\tau}_c}{\overline{h} - \frac{2N}{l_m}\tanh\left(\frac{Nl_m\overline{h}}{2}\right)}$$

and friction factor $\overline{\tau}_c$ for dominant Couette flow has been obtained by Taylor and Dowson [4] which has been later used by many researchers as given below:

$$\overline{\tau}_c = 1 + 0.00099\left(\mathrm{Re}_h\right)^{0.96} \tag{25}$$

Consequently, the friction variable is obtained as follows:

$$f\left(R/C\right) = \frac{\overline{F}}{\overline{W}} \tag{26}$$

III. Results and Discussions

The pressure distribution is taken symmetrical about the mid plane. The grid size taken in the circumferential and axial direction as 44 and 12 respectively. The convergence criteria for pressure has been taken as 0.001. The steady state pressure distribution can be calculated using equation (16). The exact comparison for turbulent flow is not available in the literature, however the trends of the results are similar to laminar flow but the values are quite increased.

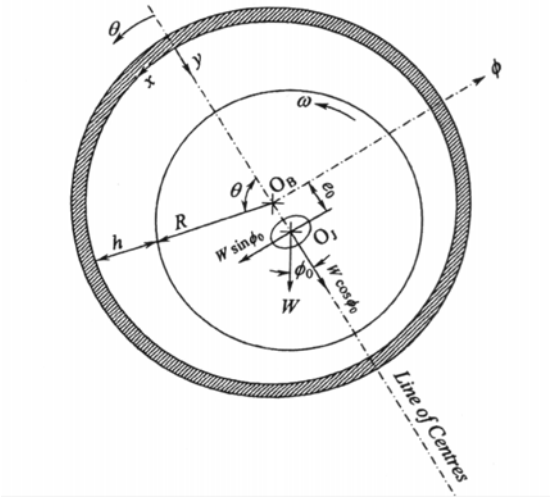

Fig. 1 Circular Bearing geometry

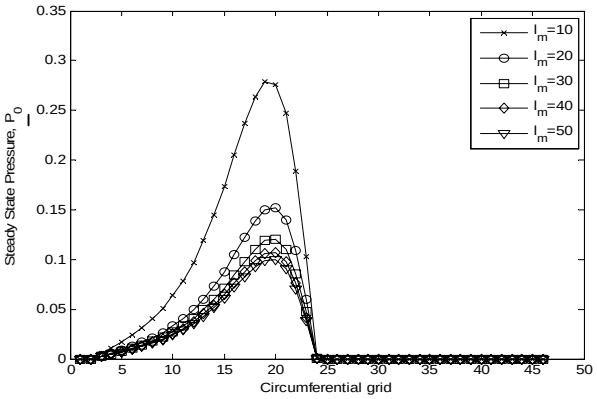

Fig. 2 Pressure variation, $\overline{p}_0$ along circumferential direction for various l_m, ε=0.5, Re=5000, N^2=0.5

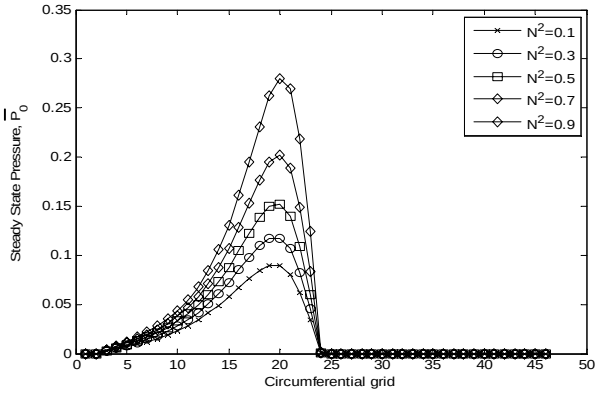

Fig. 3 Pressure variation, $\overline{p}_0$ along circumferential direction for various N^2, ε=0.5, Re =5000, l_m =10.0

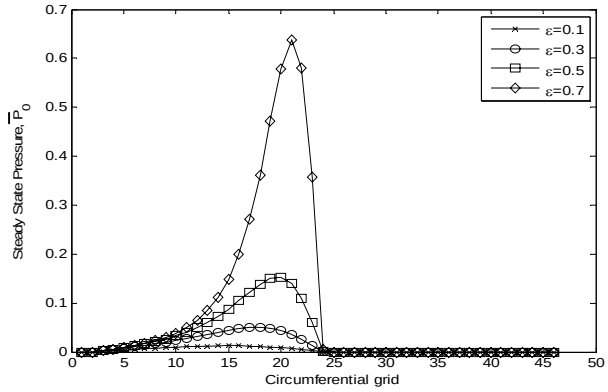

Fig. 4 Pressure variation, $\overline{p}_0$ along circumferential direction for various ε, l_m =10.0, *Re* =5000, N^2=0.5

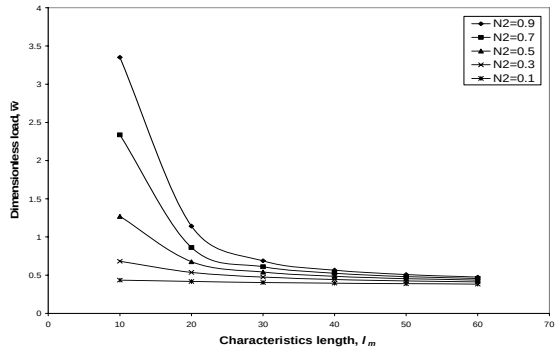

Fig. 5 Dimensionless load Vs. Characteristic length for various N^2 values, *L/D*=0.1, ε=0.5, *Re*=5000

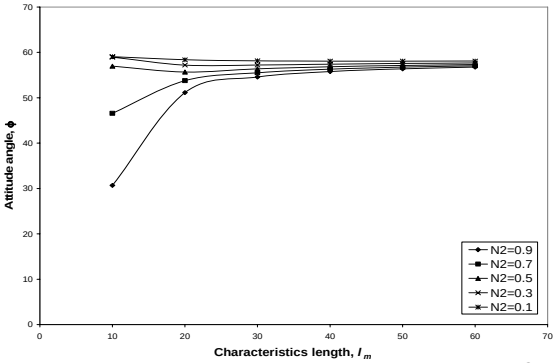

Fig. 6 Attitude angle Vs. Characteristic length for various N^2 values, *L/D*=0.1, ε=0.5, *Re*=5000

The steady state pressures for various parameters are depicted in Figs. 2 - 4. Fig. 2 shows pressure variation along circumferential direction for different characteristic lengths. It is seen that pressure is very much significant for l_m equals 10. Figure 3 shows the peak value of pressure for coupling number equals 0.9 which is in the similar trend for laminar flow condition [6-9]. The effect of higher eccentricity is also depicted in Fig. 4. It shows that pressure increases as the eccentricity ratio increases.

The effect of load capacity and attitude angle are as shown in the Figs. 5 - 11. These figures are in the same trend to that of laminar flow finite bearing solutions.

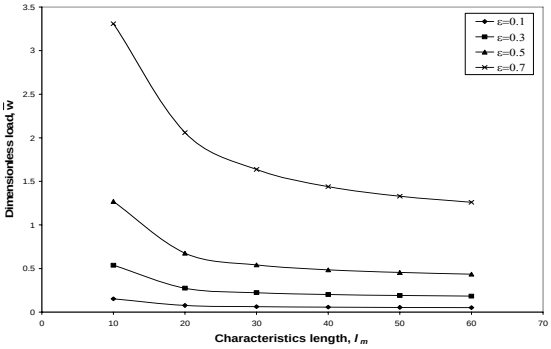

Fig. 7 Dimensionless load Vs. Characteristic length for various ε values, *L/D*=0.1, N^2=0.5, *Re*=5000

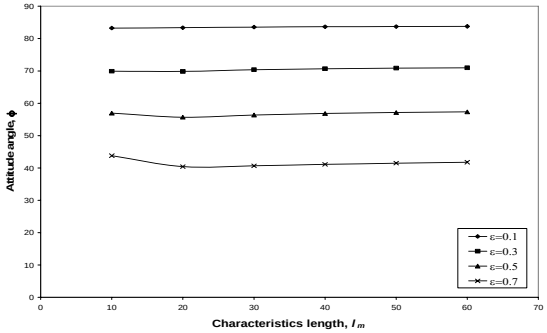

Fig. 8 Attitude angle Vs. Characteristic length for various ε values, *L/D*=0.1, N^2=0.5, *Re*=5000

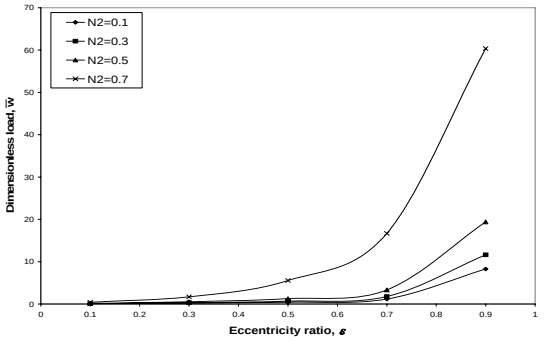

Fig. 9 Dimensionless load Vs. Eccentricity ratios for various N^2 values, *L/D*=0.1, l_m =10.0, *Re*=5000

Figure 5 shows the load carrying capacity varies as a function of l_m for a number of N^2, keeping the eccentricity ratio constant. It shows load capacity is larger for lower l_m and load approaches to Newtonian fluid as N^2 equals closer to zero. The attitude angle is lower for lower l_m as well as for higher N^2 as can be seen in Fig. 6. The load carrying capacity decreases with increase in l_m but shows higher value at higher eccentricity ratio. Whereas the attitude angle almost remains constant throughout the l_m but shows lower value at higher eccentricity ratio. Both the above mentioned trends can be visualized in the Figs. 7 & 8. Fig. 9 shows the plots of load capacity versus eccentricity ratio for different coupling number. The plot reveals that load capacity increases with increase in eccentricity as well as coupling number for a constant characteristics length equals 10.

But the attitude angle drops down with increase in eccentricity ratio for all the values of N^2 as can be seen in Fig. 10.

The friction force and friction variable versus l_m for different N^2 are plotted in Figs. 11 & 12. These curves also are in the same trend to that of laminar flow as depicted in Khonsari and Brewe [6] but the values are quite larger when compared to laminar flow. Figures 13 & 14 show the plots of friction force and friction variable versus l_m for various eccentricity ratios. The friction force has the decreasing trend whereas the friction variable has the increasing trend but similar to that of again laminar flow. Friction force increases with increase in N^2 for increasing eccentricity ratios which are depicted in Fig. 15. Variation of the coefficient of friction as a function of eccentricity is shown in Fig.16 for a number of N^2 for l_m equals 10. This figure indicates that under the conditions simulated, micropolar fluids exhibit a beneficial effect in that the coefficient of friction is lower than the Newtonian fluids which can be judged by substituting N^2 equals 0.0. Furthermore, lower friction coefficients result with increase in coupling number.

It should be noted that friction coefficient of lubricant micropolarity tends to be lower than that of the Newtonian fluids, the friction force tends to be higher. The reason for this is of course due to the load capacity of the micropolar fluids increasing more which compensates for the frictional force. This discussion and explanation is already mentioned by Khonsari and Brewe [6].

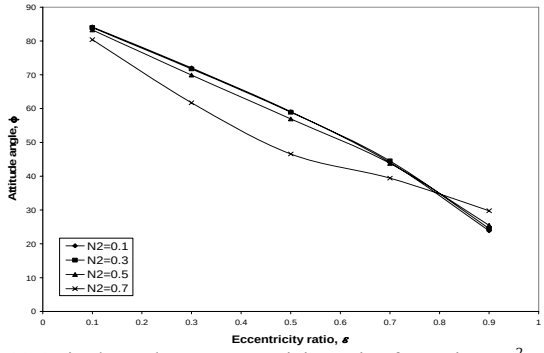

Fig. 10 Attitude angle Vs. Eccentricity ratios for various N^2 values, L/D=0.1, l_m =10.0, Re=5000

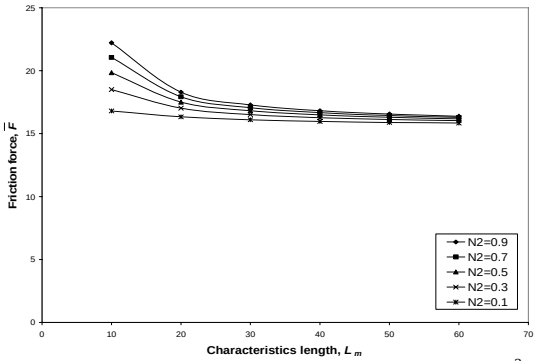

Fig. 11 Friction force Vs. Characteristic length for various N^2 values, L/D=0.1, ε=0.5, Re=5000

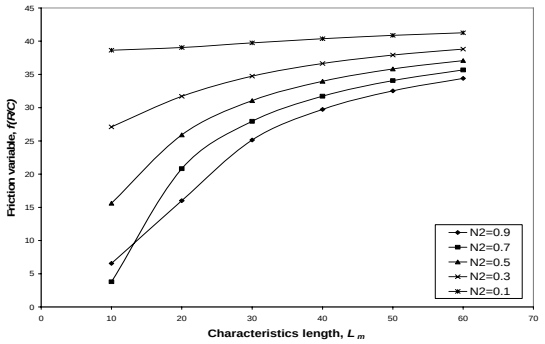

Fig. 12 Friction variable Vs. Characteristic length for various N^2 values, L/D=0.1, ε=0.5, Re=5000

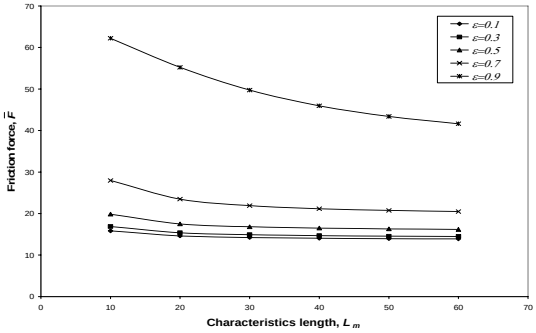

Fig. 13 Friction force Vs. Characteristic length for various ε values, L/D=0.1, N^2=0.5, Re=5000

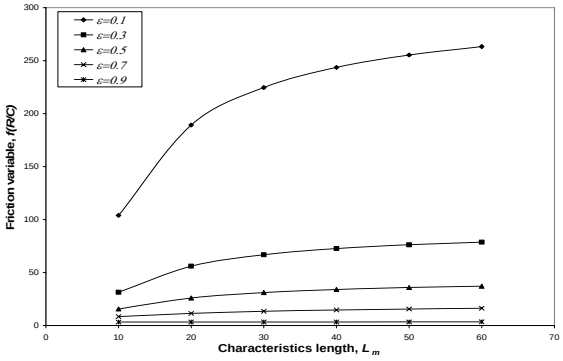

Fig. 14 Friction variable Vs. Characteristic length for various ε values, L/D=0.1, N^2=0.5, Re=5000

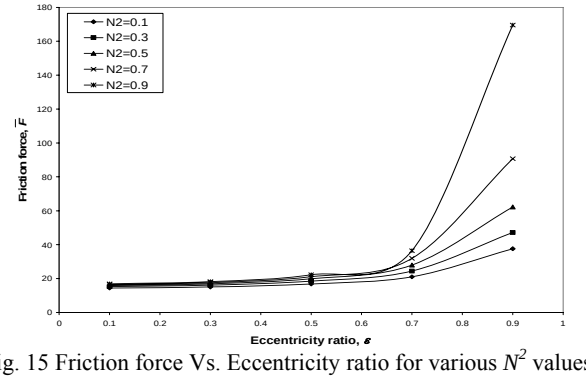

Fig. 15 Friction force Vs. Eccentricity ratio for various N^2 values, L/D=0.1, L_m=10.0, Re=5000

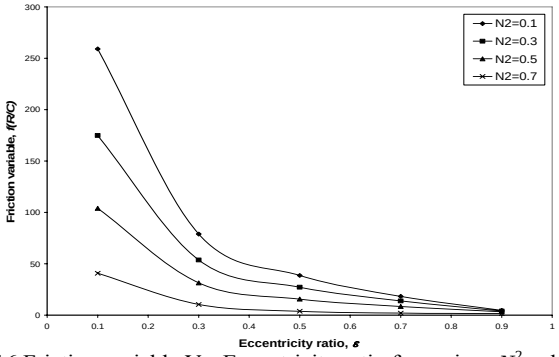

Fig. 16 Friction variable Vs. Eccentricity ratio for various N^2 values, L/D=0.1, L_m=10.0, Re=5000

IV. Conclusions

An approximate study of the lubricating effectiveness of micropolar fluids in a short journal bearing considering the turbulent flow has been presented. The results indicate that for a steadily loaded short journal bearing, the micropolar fluids do exhibit a high load carrying capacity and the friction coefficient is less than that of Newtonian fluid. Hence, micropolar fluid can also be used for turbulent flow condition.

V. Nomenclature

C Journal bearing radial clearance, m

e Eccentricity 'm', $\varepsilon = e/C$ (d'less)

$f(R/C)$ Friction variable (d' less)

F Friction force (N), $\overline{F} = FC/\mu\Omega R^2 L$ (d' less)

h Film thickness 'm', $\overline{h} = h/C$ (d'less)

h_{cav} Film thickness at the point of cavitation, $\overline{h}_{cav} = h_{cav}/C$ (d'less)

K_ζ Turbulent couette shear factor

l_m Non-dimensional characteristic length of the micropolar fluid, $l_m = \Lambda/C$ (d'less)

L Bearing length, m

N Coupling number, $N = [\chi/(2\mu+\chi)]^{1/2}$

p_0 Static fluid pressure (Pa), $\overline{p}_0 = p_0 C^2/\mu\Omega R^2$

$\overline{p}_1, \overline{p}_2, \overline{p}_3, \overline{p}_4$ Dynamic pressures (d'less)

R Radius of journal bearing, m

Re Reynolds number $(\rho CR\Omega/\mu)$, $\mathrm{Re}_h = \overline{h}\,\mathrm{Re}$

t Time (sec), $\tau = \Omega t$ (d' less)

U Linear velocity of journal centers, m/s ($U = R\omega$)

W Applied load on bearing (N), $\overline{W} = WC/\mu\Omega R^2 L$

$\overline{W}_r$ Radial component of load (d'less)

$\overline{W}_t$ Tangential component of load (d'less)

$\overline{W}$ Total d'less applied load, $\overline{W} = \sqrt{\overline{W}_r^{\,2} + \overline{W}_t^{\,2}}$

x, z Circumferential and axial coordinate axes

θ, ζ Dimensionless coordinate axis

θ_{cav} Angular coordinate where the film cavitates

μ Dynamic viscosity, Pa-s

ω Angular velocity of the journal, r/s

ϕ Attitude angle

ν Vibration frequency of the journal center (rad/s)

γ Whirl frequency ratio, $\gamma = \upsilon/\omega$ (d'less)

Λ Characteristic length of the micropolar fluid, $= (\gamma/4\mu)^{1/2}$

References

[1] V. N. Constantinescu, "Analysis of Bearings Operating in Turbulent Regime," J Basic Eng., 84(1): 474, 1962.

[2] C. W. Ng, and C. H. T. Pan, "A Linearized Turbulent Lubrication Theory," J Basic Eng., Sept: 675-688, 1965.

[3] H. G. Elrod, and C. W. Ng, "A Theory for Turbulent Fluid Films and Its Application to Bearings," ASME J Lubri Tech, July: 346-362, 1967.

[4] C. M. Taylor, and D. Dowson, "Turbulent Lubrication Theory – Application to Design," ASME J Lubri Tech, January: 36 - 47, 1974.

[5] M. K. Ghosh, and A. Nagraj, "Rotordynamic Characteristics of a Multilobe Hybrid Journal Bearing in Turbulent Lubrication," J Eng. Tribology IMechE, Part-J, 218: 61-67, 2004.

[6] M. M. Khonsari, and D. E. Brewe, "On the Performance of Finite Journal Bearings Lubricated with Micropolar Fluids," Tribology Transaction, 32: 155-160, 1989.

[7] S. Das, S. K. Guha and A. K. Chattopadhyay, "On the Steady State Performance of Misaligned Hydrodynamic Journal Bearing Lubricated with Micropolar Fluids," Tribology International, 35: 201-210, 2002.

[8] A. D. Rahmatabadi, M. Z. Mehrjardi, and M. R. Fazel, "Performance Analysis of Micropolar Lubricated Journal Bearings using GDQ Method," Tribology International, 43: 2000-2009, 2010.

[9] A. D. Rahmatabadi, M. Nekoeimehr, and R. Rashidi, "Micropolar Lubricant Effects on the Performance of Non-circular Lobed Bearings," Tribology International, 43: 404 - 413, 2010.

[10] A. D. Rahmatabadi, R. R. Meybodi, and M. Nekoeimehr, "Preload Effects on the Static Performance of Multilobe Fixed Profile Journal Bearings with Micropolar Fluids," J Eng. Tribology IMechE, Part-J, 225: 718-730, 2011.

[11] M. Faralli, and N. P. Belfiore, "Steady State Analysis of Worn Spherical Bearing Operating in Turbulent Regime with Non-Newtonian Lubricants," International Conference in Tribology, AITC-AIT, 20-22 Sept. 2006, Parma, Italy.

[12] L. Meena, S. S. Gautam, and M. K. Ghosh, "Static and Dynamic Characteristics of Short Wavy Journal Bearings," Lubrication Science, 22: 113-132, 2010.